Modular Target Acquisition model & visualization tool

Piet Bijl, Maarten A. Hogervorst & Wouter K. Vos

TNO Defense, Security & Safety: Human Factors, P.O. Box 23, Soesterberg, The Netherlands

Phone: +31 346 356 368, fax: +31 346 353 977

E-mail: piet.bijl@tno.nl, maarten.hogervorst@tno.nl, wouter.vos@tno.nl

ABSTRACT

We developed a software framework for image-based simulation models in the chain: scene-atmosphere-sensor-image enhancement-display-human observer: EO-VISTA. The goal is to visualize the steps and to quantify (Target Acquisition) task performance. EO-VISTA provides an excellent means to systematically determine the effects of certain factors on overall performance in the context of the whole chain. There is a wide number of applications in the areas of sensor design, maintenance, TA model development, tactical decision aids and R&D. The framework is set up in such a way that modules of different producers can be combined, once they comply with a standardized interface. At the moment the shell runs with three modules, required to calculate TA-performance based on the TOD (Triangle Orientation Discrimination) method. In order to demonstrate the potential of a future comprehensive visualization tool, two example calculations are carried out using two programs not yet implemented: the pcSitoS sensor simulation model and the EOSTAR scene and atmosphere model. With the examples we show that: i) pcSitoS yields a TOD comparable to that of the real sensor that is simulated, ii) performance differences between the human visual system model implemented for automated TOD measurement and a human observer are consistent over different types of sensor and may be corrected for relatively easy, and iii) simulation results of thermal ship imagery are in line with acquisition ranges predicted with the TOD model. All these results can be studied more extensively with EO-VISTA in a systematic way.

Keywords: Target Acquisition, simulation, visualization tool, atmosphere, sensor, human observer, EO-VISTA, TOD, TDA, EOSTAR

1. INTRODUCTION

Traditionally, Target Acquisition (TA) performance characterization rests on three pillars, that all need to be connected[1]: i) field performance, ii) a laboratory sensor test, and iii) a mathematical field performance prediction model. Field performance is the important measure and field tests are always required for validation purposes. In the past, the MRTD[2] was the laboratory test for thermal imagers, the MRTD curve was predicted with FLIR90/92[3], and field performance from the MRTD was predicted with ACQUIRE[4]. Current popular methods are the TOD test method[5] and model[6,7], the NVThermIP[8] model and the MTDP[9] lab test in combination with the TRM3[10] range model.

Figure 1 illustrates a typical sensor use in the field. An observer uses a sensor and display to visualize a scene. This scene may be at a considerable distance and be affected by the atmosphere. The sensor may include signal processing, coding, transmission, and decoding. On the basis of the image, the observer makes a decision (e.g. he detects a target or recognizes a target as a tank).
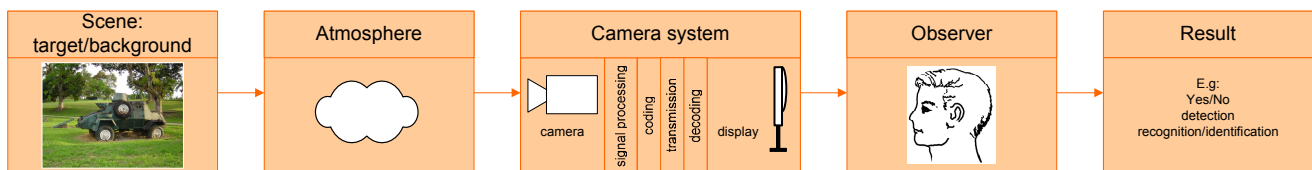

Figure 1 Typical sensor use. An observer uses a sensor and display to visualize a scene. This scene may be at a considerable distance and be distorted by the atmosphere. The sensor may include signal processing, coding,

transmission, and decoding. On the basis of the image, the observer makes a decision (e.g. he recognizes a target as a tank)

A typical lab test configuration is shown in Figure 2. A set of well-defined artificial test patterns close to the sensor replaces the real scene. A human observer (or simetimes a Human Visual System (HVS) model[6, 11]) judges the images and from his responses a lab curve is produced. The conversion from lab curve to field performance is shown in the rightmost block in Figure 2.
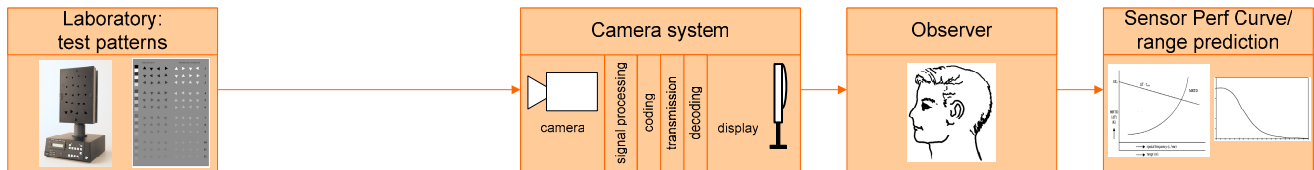

Figure 2. Typical end-to-end laboratory test configuration. The scene is replaced by as set of well-defined artificial test patterns; the test target is at short range and atmosphere plays no role. The sensor is identical to the one in the field. A human observer judges the test patterns thorugh the sensor and from his responses a lab curve is produced. Sometimes a HVS model is used instead of the observer. The rightmost block of the diagram also shows the conversion from lab curve to field performance.

In recent years, simulation has become more and more powerful, adding a variety of new possibilities with respect to visualization of the different stages in the chain from scene to observer and TA characterization. The advantage over field testing is a much better control over the circumstances and systematic parameters variation. Also hybride solutions are possible, such as using a real thermal recording of a target at short range and adding atmospheric effects using a simulation model. Of course, the other side of the coin is always that validation is required with real field data.

Currently a variety of visual simulation models from the chains in Figure 1 and Figure 2 have been developed in different laboratories. Examples are the EOSTAR[12] scene + atmosphere model, the sensor simulation models MAVIIS[13] (commercially available) and pcSitos[14] , and a TOD Human Visual System (HVS) model[6]. Until now, however, they operate in isolation, while a powerful package may be obtained once they are connected.

We developed a software framework for image-based simulation models in the chain: scene-atmosphere-sensor-image enhancement-display-human observer. The program is called EO-VISTA. The goal is to visualize the effects of consecutive steps and to quantify the consequences in terms of (Target Acquisition) task performance. The framework is set up in such a way that modules of different producers can be combined, once they comply with a standardized interface. This will enable the combination of the best available models for modeling atmospheric effects and sensor and greatly simplifies the implementation of new software versions.

Applications can be found in the areas of sensor design, maintenance, TA model development, tactical decision aids and R&D. An overview is provided in Chapter 3.

This paper is organized as follows. In Chapter 2, the model structure and the chain from scene to observer are described. Applications are listed in Chapter 3. Example calculations are given in Chapter 4. Discussion and conclusions are given in Chapter 0.

2. MODEL DESCRIPTION

2.1 GENERAL STRUCTURE

The general structure of EO-VISTA is a shell with standardized communication interface to external modules. The software is written in C++. A Graphical User Interface (GUI) is used to set the settings for each module. For the communication between EO-VISTA and the modules we make use of Automation. Automation is an inter-process

communication mechanism introduced by Microsoft and mainly used on Window platforms. It enables one application, called the Automation client, to share data with another (stand alone) application, called the Automation server, and to control that application. The Automation server can provide the client with an Automation object through a Component Object Model (COM) interface called IDispatch. This enables an Automation client to bind to a server at runtime. The software only needs the module's (server's) name to connect to it. An advantage is that the modules can run in their own process space and that they cannot interfere with each other. It is not necessary for EO-VISTA to use the source code of the Automation server. The server can be for instance a dynamically linked library generated from Matlab m-code or any other program language wrapped in an Automation object. The in- and outputs of the server have to be well-defined in order to endure proper communication with EO-VISTA.

2.2 POSSIBLE MODULES

Any step in the chain may consist of different modules, each specifically meant for a certain purpose. Figure 3 gives scene input possibilities. Figure 4 gives an example image from EOSTAR after atmospheric degradation (in false color). Figure 5 shows the steps calculated in a sensor simulation model as used by Hogervorst et al. (2001)[6]. Figure 6 shows the HVS simulation module that is able to replace the human observer in performing a TOD lab test, also taken from Hogervorst et al. (2001)[6]. Given an image containing a (degraded) triangle test pattern of certain size and contrast, the HVS module determines the most likely orientation. Finally, for TA range predictions the transition from lab performance curve to field performance (e.g. probability of correct identification versus target range) needs to be made. See Figure 7. Field performance depends largely on: target dimension, target contrast and target set-specific criteria. The TOD model uses set-specific criteria M_{75} (see Bijl et al., 2007)[7]. TA model NVThermIP uses similar criteria called V_{50}. These criteria can be converted into each other[7].

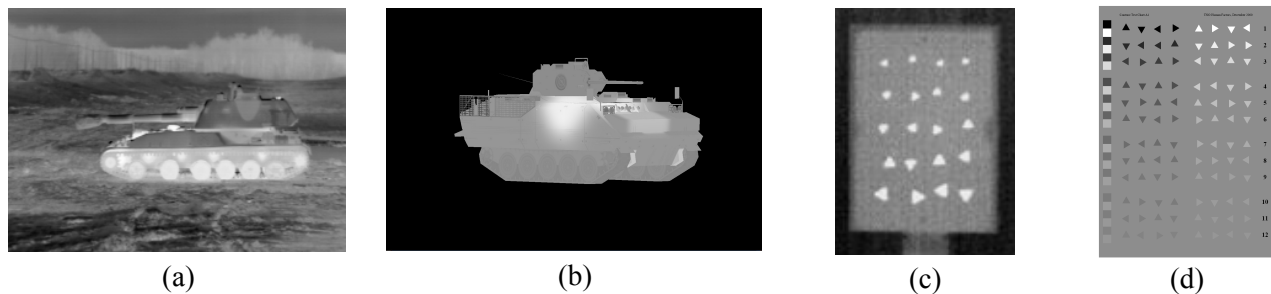| (a)	(b)	(c)	(d)

Figure 3 Scene input examples. a: pristine close-up recording of real target and background, b: simulated target, c: recorded lab test pattern, d: simulated lab test pattern
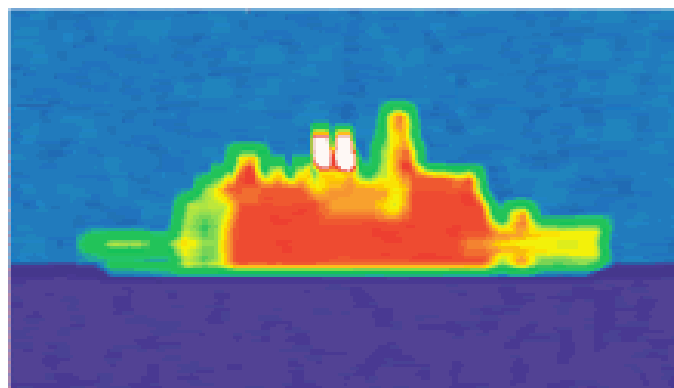
Figure 4 Example of atmospheric effects calculation with EOSTAR
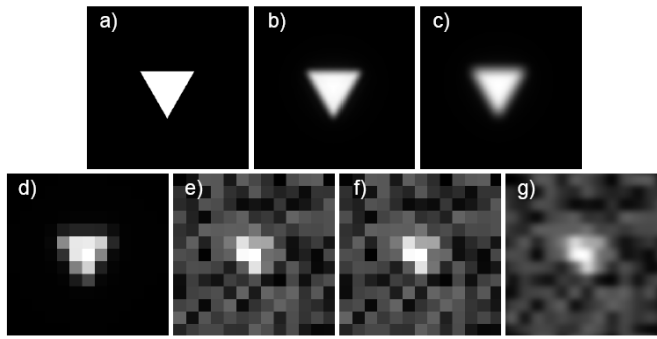
Figure 5 The image in various stages of the sensor model. From input image (a) to display image (g): a) input image, b) distorted by optics, c) after convolution with detector response function, d) sampled values, e) after addition of detector noise, f) sample & hold, g) distorted by electronics and display noise. From Hogervorst et al. (2001) [6]
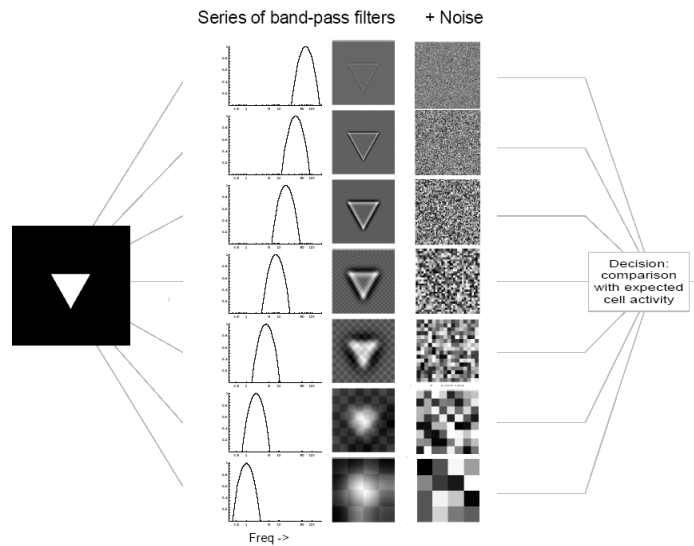

Figure 6 Biologically plausible Human Visual System module. The model compares an image containing a (degraded) triangle test pattern with 4 alternative triangle orientations and determines the most likely orientation. From Hogervorst et al. (2001) [6]
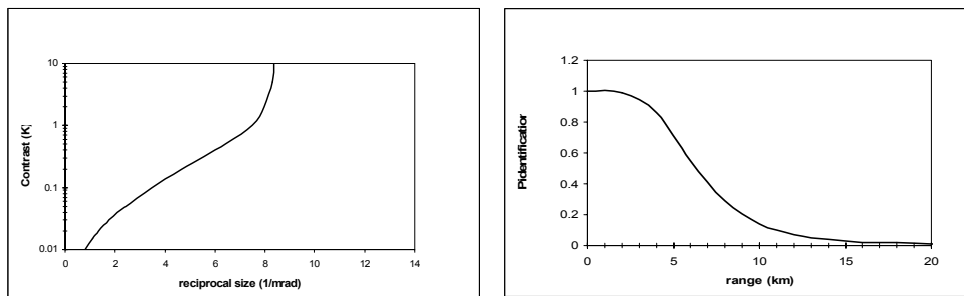

Figure 7 Field performance calculation from a lab curve. Left: TOD laboratory curve. Right: Predicted probability of correct identification as a function of target range. The acquisition range model needs: i) effective dimension and (thermal) contrast of the target set, and ii) a set-specific range criterion M_{75} related to the complexity of the

identification task. See text for details.

2.3 CURRENT IMPLEMENTATIONS

Currently, three modules have been implemented, sufficient to perform a TOD test for a simulated sensor. The three modules are: 1) a test pattern generator that produces TOD triangle test patterns of various sizes and contrasts, 2) a simple sensor simulation module from[6] (see Figure 5), and a HVS (Human Visual System) module from[6] (see Figure 6).

3. APPLICATIONS

The combination of a chain simulation on the one hand, and a simulated laboratory test with a HVS module on the other has a large number of applications. Moreover, the possibility to plug in simulated or real data anywhere increases its power. For example, it enables a direct comparison between a real and a simulated FLIR in terms of i) a visual image, ii) physical parameters such as MTF and signal-to-noise ratio and iii) psychophysical measures such as TOD performance.

Applications of the model are (not exhaustive):
- Visualization tool of all stages
- Target Acquisition range prediction
- Sensor design and/or procurement:
    - Prediction of sensor performance with the human observer or with the vision model[6]
    - Automatic characterization and optimization of image enhancement techniques[11]
    - Comparsion of competing image enhancement packages
    - Direct comparison of sensor image and sensor simulation image and a comparison in terms of (TOD) task performance.
- FAT, SAT and Maintenance:
    - Automated and human-in-the-loop TOD testing on real sensors (in combination with a lab test setup)
    - A test image generator (e.g. for CCD camera's)
- TA model validation:
    - Comparison of observer performance on real targets and TOD or any other test imagery for any simulated sensor
- R&D:
    - Systematic parameter sensitivity analysis with the complete chain modeled
    - TA model development: verify TA predictions visually and/or in terms of TA performance
    - Comparison of HVS model predictions with observer performance data on the same simulated imagery in order to improve the HVS model
    - Effects of image motion on performance
    - Comparison of different sensor simulation models
- TDA: mission preparation and training: visualization of expected imagery given the local circumstances

4. EXAMPLE CALCULATIONS

In order to illustrate the potential of a future comprehensive visualization tool, two example calculations are carried out using two programs not yet implemented: the pcSitoS[14] sensor simulation model and the EOSTAR[12] scene and atmosphere model

4.1 EXAMPLE CALCULATION 1: TOD FOR FLIR SC2000

4.1.1 INPUT PARAMETERS

The FLIR SC2000 is an uncooled LWIR microbolometer sensor with a focal plane array of 320 by 240 pixels. With the default lens the FOV is 24 by 18 degrees. The camera gives a calibrated output of the temperatures in the scene. 14 Bit

data can be digitally recorded at a frame rate of 50 Hz. The major parameters of the sensor, required to run the pcSitoS simulations, are listed in Table 1.

Table 1 Major sensor and model input parameters for the FLIR SC2000

Camera	FLIR SC2000		wavelength (μm)	7.5 - 13.0
Type	Staring, uncooled		Average optic transmission	0.8
Number of pixels	320 x 240		Focal length (mm)	36.3
H/V detector pitch (μm)	47.5		F-number	1
H/V detector size (μm)	42.5		Frame rate (Hz)	50
H/V FOV (deg)	24		NETD (K)	0.07

4.1.2   TOD FOR THE REAL FLIR SC2000 SENSOR (WITH/WITHOUT SIGNAL PROCESSING)

TOD curves for a real FLIR SC2000 were measured in a previous study[15] with the TCAT Thermal Camera Acuity Tester[16] under static and dynamic conditions with and without signal processing techniques such as dynamic super resolution (DSR). The display was a 17" CRT display at 800 x 600 pixels. It was shown in the experiment that performance was not limited by the display or eye resolution. The TOD curves consisted of 75% correct acuity thresholds at three thermal contrasts: ΔT = 16.9, 1.93 and 0.23 K, respectively. Each individual threshold estimate was calculated from 160 observer responses: 10 triangle sizes times 16 repetitions. In the experiment, four observers were used.

In the present study we will use two conditions: the still condition (a single static image), and the condition with 2x2 dynamic super resolution (indicated with DSR2). In the DSR2 condition horizontal and vertical sampling resolution is doubled resulting in a two times larger image on the display in both directions. These conditions are indicated by the 'x'-es in Table 2, second row, column 2 and 4, respectively. Since only one observer (PB) participated in the TOD experiment for the simulated FLIR in this study (see below), in the present study we will use only his results for the real sensor instead of the average over all four observers.

Table 2 Conditions for which the TOD has been determined (see 4.1.2 and 4.1.3)

observer	FLIR SC 2000		FLIR SC2000 + signal processing	
	Real (still)	Simulated (still)	Real (+ DSR2)	Simulated (+ microscan)
Real	x	x	x	x
HVS model	-	x	-	x

4.1.3   TOD FOR THE SIMULATED FLIR SC2000 SENSOR

With the pcSitoS[14] sensor simulation model (version 0.6.5.5) we simulate two sensors: the FLIR SC2000 and the same (hypothetical) sensor with 2 by 2 microscan. The sensors are indicated in the third and the rightmost column in Table 2. DSR is not an input option in pcSitoS. With micro-scan, a Focal Plane Array inside the camera is displaced every frame resulting in a higher sampling resolution. Similarly to DSR2, 2 by 2 micro-scan doubles the sampling resolution and size on the display. Hence, the result is expected to be comparable to the performance with DSR2 (see section 4.1.2).

In addition to the data from the real sensor and human observer (section 4.1.2) we produce two more TOD curves for each simulated sensor: with the human observer (Table 2, second row) , and with the HVS model observer (Table 2, bottom row). The process is shown in Figure 7. Thermal contrasts were identical to those with the real sensor (ΔT = 16.9, 1.93 and 0.23 K; see section 4.1.2). In this experiment, each threshold estimate was calculated from 210 observer responses: 7 triangle sizes times 30 repetitions. The imagery for the human observer was presented on a 17" display, large enough to avoid limitation of performance was by the display or eye resolution. Only one observer (PB) participated in this experiment.

The remaining conditions in the bottom row of Table 2 (indicated by '-') were not measured. These conditions (real sensor with HVS model) which are planned for the future, would mean an automatic TOD measurement of the real sensor.
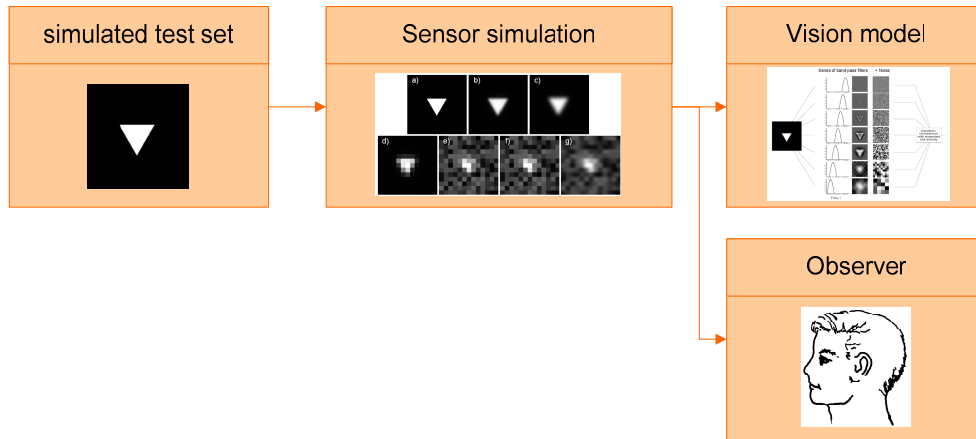

Figure 7. Simulation of the TOD measurement for the FLIR SC2000 and the hypothetical sensor with microscan. A test pattern set is fed into the pcSitoS sensor simulation model with the FLIR SC2000 sensor parameters. The output image is judged by 1) the vision module, and 2) a human observer. In addition, a real TOD measurement is carried out with the real FLIR SC2000 (normal and with super resolution applied). See text for details.

4.2 RESULTS

Table 2 shows that we have three TOD curves for each sensor. This enables us to separately i) check the quality of the sensor simulation (comparison of the scores for the human observer on the second row, see section 4.2.1) and ii) check the performance of the HVS simulation (comparison of the scores for the simulated sensors in columns 3 and 5, see section 4.2.2).

4.2.1   SIMULATED VERSUS REAL SENSOR

Figure 8 (left picture) shows an example FLIR SC2000 picture of the TCAT Thermal Camera Acuity Tester[16] with triangle test patterns of decreasing size (thermal contrast = 16.9 K). The right picture shows a pcSitoS simulation with the same test pattern sizes and thermal contrast. Note that the phases of the test patterns with respect to the sensor pixels are not matched, resulting in slightly different shapes.

Figure 8. Left: real FLIR SC2000 image of the TCAT Thermal Camera Acuity Tester. Right: pcSitoS simulation. Visual inspection indicates that there is a good agreement. See text for details
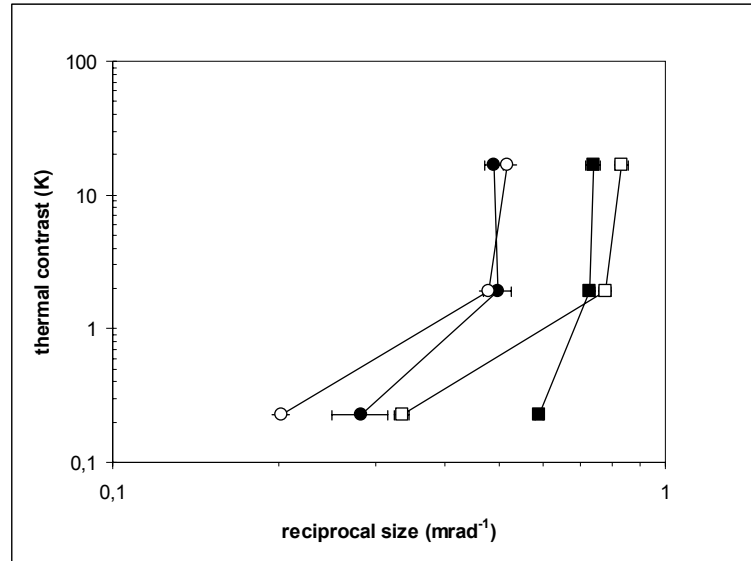

Figure 9: TOD curves for a real and simulated FLIR SC2000 camera with a human observer. Filled circles: real sensor (normal). Open circles: simulated sensor (normal). Filled squares: real sensor + DSR2. Open squares: simulated sensor + microscan. Data are plotted on log-log scales for a better comparison (TOD convention is lin-log). The results show that: i) for the normal FLIR there is a good agreement between the real and the simulated sensor: differences are small and not significant, ii) for the enhanced sensor there is a good agreement at high ΔT, iii) acuity improvement with microscan (open symbols) is 60% at all contrast levels, iv) acuity improvement with DSR2 at high ΔT is 50%, v) for the real sensor with DSR2 the behaviour at low contrast is different than for the simulated sensor with microscan. This difference can be ascribed to frame averaging applied in DSR2 (but not in our simulated microscan) resulting in a considerably lower noise level and thus a better performance at low contrasts. We conclude that the pcSitoS simulation of the camera under test results in a TOD that is comparable to that for the real sensor.

Figure 9 shows the results of the TOD measurements for a real and simulated (normal and enhanced) FLIR SC2000 camera with a human observer. Filled symbols represent the real sensor, open symbols the simulated camera. Circles represent the normal sensor, and squares the sensor with DSR and microscan, respectively. There is good agreement between the TOD for the real and simulated normal sensor, and for the enhanced sensor at high contrast. At low contrast DSR uses frame avaraging that reducces the noise, and this averaging is in our calculations not applied to microscan, and this explains the different behaviour at low contrast. We conclude that the pcSitoS simulation of the camera under test results in a TOD that is comparable to that for the real sensor.

4.2.2   SIMULATED VERSUS REAL OBSERVER

Figure 10 shows a TOD comparison between a human observer and a HOV model. It turns out that the human observer is better at the acuity level, but the model is better at lower contrasts. The prediction error is remarkably constant over sensor type indicating that a relatively simple correction of the HVS may results in a much better prediction for both well-sampled and undersamled imagers The improvement of range using microcan is 55%, close to the experimental data for real targets (60%)
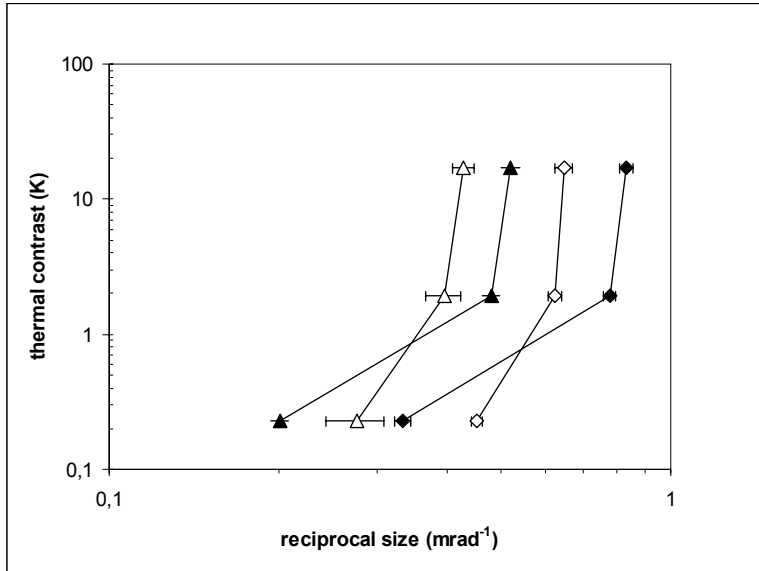
Figure 10: TOD curves with a human observer and the HVS model for the simulated sensor. Filled triangles: normal sensor + human observer. Open triangles: normal sensor + HVS model. Filled diamonds: microscan sensor + human observer. Open diamonds: microscan sensor + HVS model. Data are plotted on log-log scales for a better comparison (TOD convention is lin-log). The data show that: i) at high ΔT the human observer is better than the HVS model (18% on average), ii) at low ΔT the HVS model is better than the human observer (35% on average), iii) the results are consistent over the two sensors (note that the shapes of the curves are remarkably the same), and iv) the acuity improvement of microscan over normal with the HVS model is 55%, in agreement with the improvement with the human observer (Figure 9). We conclude that the HVS needs tuning but that the errors are identical for well-sampled and under-sampled sensors. The simulation tool is an excellent means to systematically test and improve the HVS model for a wide set of sensors.

4.2.3   SMALL CRAFT ID RANGE PREDICTIONS WITH THE TOD MODEL

In section 4.3, a simulation of a small craft thermal image with the normal and enhanced FLIR SC2000 camera will be made using a scene generator (from EOSTAR) and the pcSitoS sensor simulation model. In this section, we will perform range predictions based on the TOD curves from the section above.

In order to make a range predictions for real targets, target set characteristics such as effective target dimension and characteristic target contrast, and range criteria are required (see 2.2). Effective target dimension and target contrast are taken from the simulated craft image (see 4.3). For small craft in side view, Krapels et al (2006) provide V_{50} = 8.5. This value is converted[7] into M_{75} = 5.1 in order to make range predictions based on the TOD curves.

The results are shown in Figure 11. The predicted 75% correct ranges are 450 and 700 m, respectively.
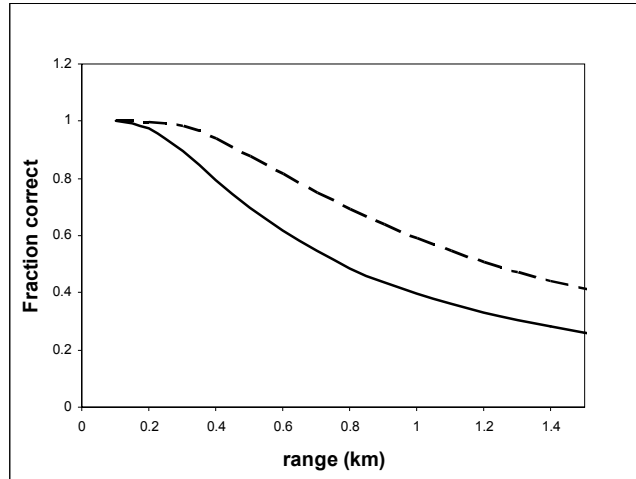
Figure 11: Identification fraction correct versus range predictions for small craft in side view made with the TOD model, based on the TOD curves for the FLIR SC2000 (normal and microscan) as determined with the HVS model (see Figure 11). The predicted 75% correct ranges are 450 and 700 m, respectively.

4.3 EXAMPLE CALCULATION 2: SHIP TARGET SIMULATION

The results of the calculation with EOSTAR and pcStoS are shwon in Figure 12. Left picture: original at the sensor, middle: normal FLIR image at 400 m distance, right: microscan-enhanced FLIR image at 640 m. According to the model calculations, these ranges should both result in an identification level of about 80%. From a subjective inspection we judge that the information content of the two sensor images is about the same. For a real conclusion it is necessary to perform an identification experiment with a set of targets.
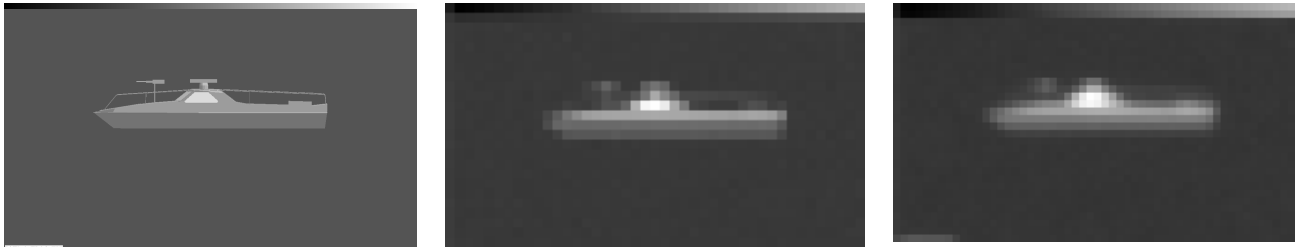

Figure 12: simulation of the FIAC small craft in side view. Left: original radiation picture generated with EOSTAR. Middle: After pcSitoS simulation of the FLIR SC2000 at 400 m (i.e. the predicted 80% correct range with the TOD model). Right: After pcSitoS simulation of the FLIR SC2000 + microscan at 640 m (i.e. the predicted 80% correct range with the TOD model). The model predicts equal identification performance for the two sensors at these ranges and this is not in contradiction with subjective judgement of the images. Actual confirmation needs to be determined in an observer experiment with more targets. The simulation model is an excellent tool to design such an experiment.

5. DISCUSSION AND CONCLUSIONS

We provide a software framework for image-based simulation models in the chain: scene-atmosphere-sensor-image enhancement-display-human observer. The goal is to visualize the steps and to quantify (Target Acquisition) task performance.

The model provides an excellent means to systematically determine the effects of certain factors on overall performance in the context of the whole chain.

The program has a wide number of applications in the areas of sensor design, maintenance, TA model development, tactical decision aids and R&D. Currently the applicability is limited because there are only three modules implemented.

In order to demonstrate the potential of a future comprehensive visualization tool, we perform two off-line example calculations using two programs not yet implemented. These (limited) calculations show how well the sensor simulation program and the HVS model perform, and whether the quality of simulated ship images at certain range correspond to the prediction of the models.

The tool enables a much more extensive test, e.g. a real ID test with:
- more targets and more orientations
- a simple or complex atmosphere
- sensor parameter variation (spectral as well)
- simulated motion (target or sensor)
- signal processing

At the same time, TOD and range can be predicted, indicating how robust the method is over large variation of input parameters

ACKNOWLEDGMENT

REFERENCES

1. Driggers, R.G., Vollmerhausen, R., Wittenstein, W., Bijl, P., Valeton, J.M. (2000). Infrared Imager Models for Undersampled Imaging Systems. Proc. Fourth Joint International Military Sensing Symposium, 45, 1, 335-346.
2. NATO, ''Measurement of the minimum resolvable temperature difference MRTD of thermal cameras,'' STANAG 4349, NATO, Brussels, Belgium (1995).
3. Ratches, J.A. (1976). Static Performance Model for Thermal Imaging Systems. *Optical Engineering*, 15, 6, 525-530, 1976.
4. Ratches, J.A., Vollmerhausen, R.H., Jacobs, E., & Driggers, R.G. (2001)Target acquisition performance modeling of infrared imaging systems: past, present, and future," IEEE Sensors Journal **1**, 31-40 (2001).
5. Bijl, P.& Valeton, J.M. (1998). TOD, the alternative to MRTD and MRC. Optical Engineering 37, 7, 1976 - 1983.
6. Hogervorst, M.A., Bijl, P. & Valeton, J.M. (2001). Capturing the sampling effects: a TOD sensor performance model. SPIE Proceedings Vol. 4372, 62-73.
7. Bijl, P. & Hogervorst, M.A.(2007). NVThermIP vs TOD: matching the Target Acquisition range criteria. SPIE Proceedings 6543, pp. 65430C.
8. Vollmerhausen, R., & Driggers, R.G (1999). NVTherm: next generation night vision model. Proc. IRIS Passive Sensors, 1, 121-134.
9. Wittenstein, W. (1999). Minimum temperature difference perceived – a new approach to assess undersampled thermal imagers. Optical Engineering 38, 5, 773 – 781.
10. Wittenstein, W., Fick, W. & Raidt, U. (1996). Range Performance of Two Staring Imagers - Presentation of the Field Trial and Data Analysis. Proc. SPIE Conf. on Infrared Imaging Systems, 2743, 132, (1996).
11. De Lange, D.J., Valeton, J.M. & Bijl, P. (2000). Automatic characterization of electro-optical sensors with image-processing, using the Triangle Orientation Discrimination (TOD) method. SPIE Proceedings, Vol. 3701, 104-111.
12. Kunz, Gerard J.; Degache, Marianne A. C.; Moerman, Marcel M.; van Eijk, Alexander M. J.; Neele, Filip P.; Doss-Hammel, Stephen M.; Tsintikidis, Dimitri (2004). Status and developments in EOSTAR, a model to predict IR sensor performance in the marine environment. Proceedings of the SPIE, Volume 5572, pp. 101-111

13. 13. MAVIISS (MTF-based visible and infrared imaging system simulation) software is available from JCD Publishing, 2932 Cove Trail, Winter Park, FL 32789. See www.JCDPublishing.com
14. Wittenstein, W. (2006). pcSITOS User's Guide and model description. Report FGAM-FOM, Ettlingen, Germany.
15. Bijl, P., Schutte, K. & Hogervorst, M.A. (2006). Applicability of TOD, MRT, DMRT and MTDP for dynamic image enhancement techniques. SPIE Proceedings 6207
16. Valeton, J.M., Bijl, P., Agterhuis, E. & Kriekaard, S. (2000). T-CAT, a new Thermal Camera Acuity Tester. *SPIE Proceedings Vol. 4030*, 232 – 238.